Title: The memory of airway epithelium damage in smokers and COPD patients.

Authors: François M. Carlier[1,2,3], MD PhD; Bruno Detry[1]; Marylène Lecocq[1]; Amandine M. Collin[1], PhD; Thomas Planté-Bordeneuve[1], MD; Stijn E. Verleden[4], PhD; Claudia M. Stanciu-Pop[5], MD; Benoît Rondelet[3,6], MD PhD; Wim Janssens[4], MD PhD; Jérôme Ambroise[7], PhD; Bart M. Vanaudenaerde[4], MD PhD; Sophie Gohy[1,8], MD PhD; and Charles Pilette[1,8*], MD PhD.

Affiliations:

[1]Pole of Pneumology, ENT, and Dermatology, Institute of Experimental and Clinical Research, Université Catholique de Louvain, Brussels, Belgium

[2]Department of Pneumology, CHU Mont-Godinne UCL Namur, Yvoir, Belgium

[3]Lung Transplant Centre, CHU Mont-Godinne UCL Namur, Yvoir, Belgium

[4]Department of chronic diseases, metabolism and ageing, Katholieke Universiteit Leuven, Leuven, Belgium

[5]Department of Pathology, CHU Mont-Godinne UCL Namur, Yvoir, Belgium

[6]Deparment of Cardiovascular and Thoracic Surgery, CHU Mont-Godinne UCL Namur, Yvoir, Belgium.

[7]Centre de Technologies Moléculaires Appliquées, Institute of Experimental and Clinical Research, Université catholique de Louvain, Brussels, Belgium;

[8]Department of Pneumology, Cliniques Universitaires St-Luc, Brussels, Belgium

***Corresponding author**

Charles Pilette, MD PhD

Pole of Pneumology, ENT, and Dermatology

Institut de Recherche expérimentale et clinique (IREC)
Université Catholique de Louvain
Tour Claude Bernard +5
Avenue Hippocrate, 54
Bte B1.54.04
1200 Brussels
Belgium
Phone : +3227649449
Fax : +3227649440
charles.pilette@uclouvain.be

Author contributions

F.M.C. performed experiments, most data analysis, co-supervised the experimental design and wrote the manuscript. B.D. helped with cell cultures and samples collection. M.L. processed samples, designed PCR primers and performed some PCR. T.P.B., W.J. and B.M.V. revised the manuscript. S.E.V., C.M.S. and B.R. collected and provided samples. J.A. performed single cell RNA sequencing analysis. A.M.C. helped with cell cultures. S.G. helped with manuscript redaction and revision. C.P. supervised the design of the study and the writing of the manuscript.

Acknowledgements. The authors would like to thank J. Van Snick for his help with IL-6 ELISA, V. Lacroix and D. Hoton for providing surgical tissue, A. Daumerie for technical advices, M. de Beukelaer and Ch. Fregimilicka for their help with samples processing, and the IREC Pole of Microbiology (UCLouvain, Brussels, Belgium) for sharing their molecular biology facility. They also warmly thank Pr. Y. Yamamoto and his team (Jikei University School of Medicine, Tokyo, Japan) for sharing their single-cell RNA-sequencing data, not yet publicly available at the time of submission.

Sources of support. This work was supported by the Fondation Mont-Godinne, Belgium, grant to FC (N°FMG-2015-BC01, FMG-2016-BC01, and FMG-2017-BC01) and by the Fonds National de Recherche Scientifique (FNRS), Belgium, grant to FC (N°1.L505.18) and to CP (N°1.R016.16 and 1.R016.18). Funders were not involved in study design, data collection, data analysis, interpretation, or writing of the manuscript.

Competing interests. The authors have nothing to disclose.

Correspondence and requests for materials should be addressed to C.P. (charles.pilette@uclouvain.be)

Running title: Memory of airway epithelium pathology in COPD

Word count: XXX

Abstract.

Background. Chronic obstructive pulmonary disease (COPD) is a devastating lung disease, representing the third cause of mortality worldwide. In COPD, the bronchial epithelium displays several structural and functional abnormalities affecting barrier integrity, cell polarity, and differentiation, as well as epithelial-to-mesenchymal transition (EMT) and inflammation. Although COPD is currently considered an irreversible disease, the (ir)reversible nature of epithelium changes *ex vivo* remains poorly known.

Methods. The persistence of COPD epithelial abnormalities was addressed in very long-term (10 weeks) primary cultures of air/liquid interface (ALI)-reconstituted airway epithelium from non-smoker controls, smoker controls, and COPD patients. The role of inflammation was also explored by stimulating ALI cultures with a cytokine mix consisting of TNF-α, IL-6 and IL-1β. Finally, the cellular niche holding epithelial memory was studied by exploiting a single cell RNA-sequencing database.

Results. Almost all epithelial defects (barrier dysfunction, impaired polarity, lineage abnormalities) observed in smokers and COPD patients persisted *in vitro* up to week 10, except IL-8/CXCL-8 release and EMT which declined over time. Cytokine treatment induced COPD-like changes and reactivated EMT in COPD cells. Progenitor cells of large and small airways, namely basal and club cells, exhibited EMT-related signatures reminiscent of features observed *in situ*.

Conclusions. The airway epithelium from smokers and COPD patients displays a memory of its native state and previous injuries by cigarette smoking, which is multidimensional and sustained for years. This memory probably resides in progenitor cells of the airway epithelium.

Abstract word count. 235

Key words. COPD, epithelial memory, airway epithelium, barrier dysfunction, EMT, inflammation, pIgR

Introduction

Chronic obstructive pulmonary disease (COPD) currently represents the third leading cause of death worldwide (1). The key factors underlying this pathology are the exposure to noxious airborne stimuli, most importantly cigarette smoke (CS), and genetic predisposition (2). COPD is characterized by a progressive and mostly irreversible airway obstruction related to the narrowing and disappearance of small conducting airways (3) and the destruction of the alveolar walls, referred to as emphysema (4). The irreversible nature of the disease also refers to the relatively modest effects of currently available therapies (5) including inhaled corticosteroids and bronchodilators, none of which targeting the underlying pathways leading to structural remodeling of the lungs.

The airway epithelium (AE) acts as a first line barrier against inhaled particles and antigens and is as such constantly exposed to airborne pollutants. This AE fulfills multiple functions to maintain pulmonary homeostasis, ensuring adequate barrier function, cell differentiation and polarization, and maintaining a tight control on inflammatory mechanisms.

In COPD, AE structure and biology are profoundly altered, impacting those core epithelial functions. Indeed, the functionality and composition of the COPD bronchial epithelium is modified, notably with altered physical barrier function (6, 7) underpinned by decreased bronchial expression of tight and adherens junction (TJ and AJ) proteins such as zonula occludens-1 (ZO-1) and E-cadherin (8), and abnormal differentiation with decreased function and numbers of ciliated cells (9, 10), diminished club cells numbers and club cell secretory protein (SCGB1A1) production (11, 12) and hyperplastic goblet cells, the latter being possibly more related to CS exposure than to the disease *per se* (13). In parallel with these anomalies, the COPD AE also displays aberrant epithelial-to-mesenchymal transition (EMT), that is triggered by CS in a TGF-β-dependent manner (14) and further enhanced in COPD, both in

large and small airways (15), contributing to subepithelial fibrosis and cancer susceptibility in COPD patients (16)

The AE also expresses the polymeric immunoglobulin receptor (pIgR), which is considered a marker of epithelial polarization (17, 18) and constitutes a key component in local immune mechanisms (19-21). The pIgR ensures the transcytosis and release of subepithelial polymeric immunoglobulins (Ig) into mucosal secretions through epithelial transcytosis, a process finalized by the cleavage of pIgR at the apical side of the epithelium. This results in the secretion in the airway lumen of its extracellular part, the secretory component (SC), either free or bound to polymeric Ig thereby generating secretory (S-)Ig (19). The pIgR/SC system is defective in the COPD AE with decreased epithelial pIgR expression (17) and local S-IgA deficiency in small airways being associated with epithelial inflammation and remodeling (22, 23).

Finally, epithelial inflammation is a paramount feature in COPD and is thought to represent a major player in the disease pathophysiology (24). In line with the increased presence of intraepithelial neutrophils (25), increased levels in tumor necrosis factor (TNF)-α, interleukin-8/C-X-C Motif Chemokine Ligand 8 (IL-8/CXCL-8) and neutrophils have been observed in sputum from COPD patients (26, 27) and correlate with disease severity (28).

The air/liquid interface (ALI) culture model of primary human bronchial epithelial cells (HBEC) allows the reconstitution of the AE *in vitro* and has been shown to recapitulate several of the observed alterations in the native tissue. Indeed, CS extract-exposed COPD human bronchial epithelial cells (HBEC) show decreased E-cadherin and ZO-1 expression when compared with HBEC from smokers (14) and the *ex vivo* reconstituted epithelium issued from COPD patients displays features of altered lineage differentiation, decreased pIgR expression and EMT, up to 4 weeks after reconstitution (8, 10, 17). Although these data point towards the persistence of AE abnormalities in this primary cell culture model, it remains unclear whether (and to what extent) these structural changes are persistent in COPD on the long-term, matching

the irreversible nature of the disease. Heterogeneous data exist regarding this matter as, on the one hand, clinical studies show that COPD patients who quit smoking for more than 3.5 years display less goblet cell hyperplasia and squamous metaplasia (29), and that smoking cessation may slightly improve pulmonary function tests (30) and reduce mortality (31). On the other hand, smoking cessation does not influence COPD-related epidermal growth factor receptor (EGFR) activation (29) and protease activity (32). In COPD, the inflammatory pattern that is shared with 'healthy' smokers is amplified and persists even after smoking cessation (33), although data are conflicting between studies (30, 33, 34). The present study aimed to elucidate whether AE changes are imprinted in a persistent manner, or whether some changes could be reversible, i.e. questioning the memory (31) retained in epithelial cells from COPD patients.

To address this question, the AE was reconstituted in the ALI culture model with primary HBEC from non-smokers, non-COPD smokers (referred to as "control smokers") and COPD patients, and cultured *in vitro* for up to 10 weeks, and the spontaneous evolution of abnormalities was assayed for multiple readouts, namely barrier function, cell differentiation, EMT, pIgR/SC-related polarity and production of inflammatory cytokines. In addition, it was assessed whether exogenous inflammation may trigger COPD-related changes in this model. Existing single-cell RNA sequencing (scRNAseq) databases were finally exploited to identify cell populations that may retain signatures underlying the memory of epithelial damage in COPD.

Materials and methods

Study population and lung tissue samples

A series of lung surgical specimens containing large airways was obtained from four different patients' groups (non-smokers, smoker controls, mild and moderate COPD and severe to very severe COPD). COPD patients were sorted on basis of their pulmonary function tests, according to the GOLD 2001 classification (35). Surgical tissue from lobectomies was used for controls and mild or moderate COPD patients undergoing lung surgery for a solitary tumor, while explants were obtained to analyze lung tissue from patients with (very) severe COPD. Patients with any other lung disease than COPD (e.g., asthma, lung fibrosis) were excluded from the study. All patients received information and signed a written consent to the study protocol, which was approved by the local clinical Ethical committee (reference 2007/19MARS/58 for UCLouvain, S52174 and S55877 for KULeuven). A primary proximal bronchial epithelium was reconstituted *in vitro* from all subjects, and was subjected to mid-term (5 weeks, n_1=51) or long-term (10 weeks, n_2=26) culture. Patients' characteristics are shown in Tables 1, S1 and S2.

In vitro reconstitution of primary human bronchial epithelium on ALI culture

A large piece of cartilaginous bronchus was selected from lobectomies or explants, located as far as possible from the tumor site (in the case of lobectomies) and submitted to pronase digestion overnight at 4°C, in order to derive HBEC. HBEC were cultured in flasks in retinoic acid-supplemented Bronchial Epithelial Cell Growth Basal Medium (BEBM, Lonza, Verviers, Belgium) until confluence. Cells were then detached and seeded at a density of 80,000 cells/well on 24-well polyester filter-type inserts (0.4-µm pore size; Corning, Corning, NY) coated with 0.2 mg/ml collagen IV (Sigma-Aldrich, Saint-Louis, MO) until a confluent monolayer was obtained. The culture was then carried out in ALI for 5 (for 25 subjects) or 10 weeks (for 26 subjects). Once in ALI, HBEC were cultured in BEBM:Dulbecco's Modified Eagles Medium

(DMEM) (1:1) medium supplemented with penicillin (100U/ml), streptomycin (100µg/ml) (Lonza, Verviers, Belgium), bovine serum albumin (BSA) (1.5 µg/ml), retinoic acid (30ng/ml) (Sigma, Saint-Louis, MO), and BEGM SingleQuotsTM Supplements and Growth Factors (Lonza), including bovine pituitary extract (52µg/ml), insulin (5µg/ml), hydrocortisone (0.5g/ml), transferrin (10µg/ml), epinephrine (0.5µg/ml), epidermal growth factor (0.5ng/ml) and triiodothyronine (3.25ng/ml). Every week during ALI culture, basolateral media were collected, and the apical pole of HBEC was washed with 300µl sterile phosphate-buffered saline (PBS) before centrifugation for 5 minutes at 10,000g. Transwell inserts were fixed by direct immersion in 4% buffered formaldehyde, before incubation in PBS (pH 7.4) and embedding in paraffin blocks. ALI-HBEC were also processed for mRNA abundance or Western blot analyses (see below).

The 25 samples that underwent 5 weeks ALI culture were exposed or not (control condition) to a pro-inflammatory cytokine cocktail including IL-1β, IL-6, TNF-α, each at 5 ng/ml (Miltenyi Biotec, Germany) in the basolateral compartment following a preliminary titration experiment (10, 5, and 2,5 ng/ml) where no cytotoxicity (release of lactate dehydrogenase < 5%) was shown at 5 ng/ml (data not shown).

Measurement of the transepithelial electric resistance

Every week and for each sample, the transepithelial electric resistance (TEER) of the reconstituted epithelium was assessed, using the EMD Millipore™ Millicell-ERS Volt-Ohm Meter (Fisher Scientific, Hampton, NH, USA) after transiently filling the apical pole of the cells with sterile PBS. TEER was measured in duplicates and the mean of the measurements was used, after values were corrected for the resistance of the transwell membrane.

Reverse transcriptase quantitative polymerase chain reaction (RT-qPCR)

RNA extraction, reverse transcription, and RT-qPCR were performed as previously described (36). Total RNA was extracted from reconstituted ALI cultured epithelia using TRIzol reagent (Thermo Fisher Scientific). 500ng of RNA was reverse-transcribed with RevertAid H minus Reverse transcriptase kit with 0.3 µg of random hexamer, 20U of RNase inhibitor and 1mM of each dNTP (Thermo Fisher Scientific, Waltham, MA) following the manufacturer's protocol in a thermocycler (Applied Biosystems, Foster City, CA). The expression levels were quantified by real-time quantitative PCR with the CFX96 PCR (Bio-Rad, Hercules, CA). The reaction mix contained 2.5 µl of complementary desoxyribonucleic acid diluted 10-fold, 200nM of each primer (primers properties are detailed in Table S3) and 2x iTaq UniverSybr Green® Supermix (Bio-Rad) in a final volume of 20 µl. The cycling conditions were 95°C for 3 minutes followed by 40 cycles of 95°C for 5 seconds and 60°C for 30 seconds. To control the specificity of the amplification products, a melting curve analysis was performed. The copy number was calculated from the standard curve. Data analysis was performed using Bio-Rad CFX software (Bio-Rad). Expression levels of target genes were normalized to the geometric mean of the values of 3 housekeeping genes (RPL27, RPS13, RPS18).

Western blot assays

HBEC lysates were analyzed by Western blot as previously described (37) except for band revelation (see below). Cells were lyzed with 150µl of Laemmli's sample buffer containing 0.7M 2-mercaptoethanol (Sigma-Aldrich) and lysates were stored at -20°C. After thawing, samples were heated at 100°C for 5 minutes, loaded in a SDS-PAGE gel before migration at 100V for 15 minutes and then at 180V for 50 minutes. Cell proteins were transferred onto a nitrocellulose membrane (Thermo Fisher Scientific) at 0.3A for 2 hours 10 minutes at RT. The membranes were blocked with 5% w/v BSA (Sigma-Aldrich) in Tris-buffered saline with 0.1% Tween 20 (Sigma-Aldrich) for 1 hour at RT, then washed and incubated overnight at 4°C with a primary antibody according to the target protein (see Table S4 listing used primary and

secondary antibodies). Membranes were then incubated for 1 hour at room temperature (RT) with horseradish peroxidase (HRP)-conjugated secondary anti-rabbit (Cell Signalling, Danvers, MA) or anti-mouse (Sigma) IgG. Immunoreactive bands were revealed by chemiluminescence (GE Healthcare, Pittsburgh, PA), detected by Chemidoc XRS apparatus (Bio-Rad) and quantified using the Quantity One software (Bio-Rad).

Sandwich enzyme-linked immunosorbent assay (ELISA) for SC, IL-8/CXCL-8 and IL-6

SC concentration was determined in apical washes by sandwich ELISA, as previously described (11, 37). Basolateral IL-8/CXCL8 and IL-6 release were assessed by sandwich ELISA, following manufacturer's instructions (Biotechne, Minneapolis, MN). Briefly, 96-well plates were coated overnight, at 4°C, with anti-IL-8/CXCL8, -IL-6, and -SC antibodies diluted in bicarbonate buffer (pH 9,6). Then, after blocking with 1% w/v BSA in phosphate-buffered saline for 90 min at 37°C, HBEC apical washes (for SC) or basolateral supernatants (for IL-8/CXCL-8 and IL-6) were incubated for 60 min at 37°C, along with standard samples. Detection was performed with a first incubation with the corresponding biotinylated antibody (anti-fibronectin, -SC, -IL-8/CXCL-8 or -IL-6), followed by a second incubation with HRP-linked anti-mouse IgG, for 1 h each. Revelation was performed with 3,3',5,5'-tetramethylbenzidine (TMB, Fisher) and stopped with H_2SO_4 1.8 M.

Direct ELISA for fibronectin

Fibronectin basolateral release was assessed by direct ELISA as previously described (8, 38). HBEC basolateral washes and fibronectin standard were coated in plates with bicarbonate buffer overnight (pH 9,6), at 4°C. After blocking with 1% w/v BSA in phosphate-buffered saline for 90 min at 37°C, detection was performed with a first incubation with mouse anti-fibronectin, followed by a second incubation with HRP-linked anti-mouse IgG, for 1 h each. Revelation was performed with TMB and stopped with H_2SO_4 1.8 M.

Single-cell RNA sequencing database analysis

Data from a recent single-cell RNA sequencing study were downloaded. In that study, COPD pathogenesis was analyzed in COPD patients, non-COPD smokers and never-smokers in order to investigate the disease progression at single-cell resolution (39). Data from this study were imported and analyzed into R using the R software package Seurat v.3.1.5 and the source code made available by the author on Github (https://github.com/JunNakayama/scRNAseq-COPD). In that respect, normalization, scaling, clustering of cells and identifying cluster marker genes, were performed with the same parameter than in the corresponding study. Progenitor cells of the airways (namely basal and club cells) were then selected, and EMT-related genes (VIM, FN1, SNAI1, SNAI2, S100A2, S100A4) were specifically assessed for a more comprehensive analysis.

Statistical analysis

Results were analyzed with JMP® Pro, Version 14 (SAS Institute Inc., Cary, NC, USA) and GraphPad Prism version 8.0.2 for Windows (GraphPad Software, La Jolla, CA, USA), and were expressed as medians and interquartile ranges unless otherwise stated. p-values < 0.05 were considered statistically significant.

Results

Readouts were assessed at different timepoints according to sample availability, that are referred to as "early" (1 week ALI), "short term" (2-3 weeks ALI), "mid-term" (4-7 weeks ALI) and "long-term" (8-10 weeks ALI) cultures.

Barrier and junctional properties in the COPD vs control AE

As physical barrier constitutes a first-line defense provided by the AE, this function was first assessed for impairment in COPD by measuring the transepithelial electric resistance (TEER) of ALI-reconstituted primary AE cultured for 5 weeks (n_1=51 patients) or up to 10 weeks (n_2=26 patients). According to their smoking status and lung function (GOLD 2001 classification (35)), the study population was divided into 4 groups: non-smoker controls (NS; n_1=10 for 5 weeks and n_2=5 for 10 weeks), smoker controls (Smo; n_1=15 and n_2=7), mild and moderate COPD (COPD GOLD 1-2; n_1=13 and n_2=7) and severe to very severe COPD (COPD GOLD 3-4; n_1=13 and n_2=7). The characteristics of the complete study population are summarized in Table 1, and detailed analysis of separate populations is provided in Tables S1 and S2.

The reconstituted AE from COPD patients displayed substantially decreased TEER as compared with that of non-smoker controls, and to a lesser extent with that of smoker controls (Figure 1). In addition, smoker controls AE also showed decreased TEER compared with that of non-smoker controls. This defect appeared in early ALI cultures and was progressively more prominent over time (Figure 1A-D), persisting in long-term cultures (Figure 1F). In short-term up to long-term ALI-AE, TEER inversely correlated modestly but significantly with the disease severity witnessed by the forced expiratory volume in one second (FEV1) (as represented at mid-term in Figure 1E).

To elucidate the molecular substratum of this long-lasting barrier disruption, mRNA abundance and protein expression of major components of the tight and adherens junctions were assayed,

namely claudin-1 (*CLDN1*), E-cadherin (*CDH1*), occludin (*OCLN*) and ZO-1/tight junction protein 1 (*TJP1*). Although no difference was observed between groups regarding mRNA abundance (Figure S1), protein expression of E-cadherin was reduced in COPD as compared with non-smoker controls in early and short-term ALI cultures, but not at mid-term and long-term (Figure 2A-D), while that of occludin was decreased in short-, mid- and long-term ALI-AE from smokers and COPD patients (Figure 2E-G), and inversely correlated with the disease severity, assessed by the FEV1 (as represented at mid-term in Figure 2H). Figure 2I and 2J show representative blots for E-cadherin (early and short-term) and occludin (mid- and long-term) in reconstituted AE from non-smokers and severe COPD.

These data globally depict a defect in the barrier function of the AE that is engaged in smokers, further worsens in COPD following disease severity, and which is persistent in prolonged *in vitro* culture.

Epithelial differentiation of the COPD vs control AE

In order to assess the persistence of the abnormal programming of epithelial differentiation in COPD, specific markers and transcription factors of early differentiation, intermediate, goblet, club and ciliated cells were assayed in long-term ALI cultures.

Epithelial pre-differentiation

mRNA abundance of MYB Proto-Oncogene (*MYB*), a recently described marker of early differentiation of basal cells (37), was significantly decreased up to long-term in smokers- and COPD-derived AE as compared with non-smokers (Figures 3A and S2A). In addition, *MYB* mRNA levels in early, short-term, mid-term and long-term cultures correlated with disease severity in terms of FEV1 (Figures 3D and S2A).

Differentiation towards ciliated cells

It was next assessed whether the defect in ciliated cell numbers classically observed in COPD persisted in long-term ALI cultures by measuring the mRNA abundance of Forkhead Box J1 (*FOXJ1*), a transcription factor involved in the commitment towards ciliated cells, and of the dynein axonemal intermediate chain 1 (*DNAI1*), a marker of terminal differentiation of ciliated cells. Smokers- and COPD-derived cultures displayed a marked and persisting mRNA level decrease of both targets as compared with non-smoker controls (Figures 3B-C and S2B-C). This decrease significantly correlated with disease severity (assessed by FEV1) in early, short-term, and long-term ALI culture (Figures 3D and S2B-C).

Differentiation towards goblet cells

We next assessed the mRNA abundance of SAM Pointed Domain Containing ETS Transcription Factor (*SPDEF*) and Forkhead Box A3 (*FOXA3*), two transcription factors inducing the differentiation towards goblet cells (40-42). On one hand, *SPDEF* expression was increased in smoker controls' AE (and in COPD AE, although to a lesser, non-significant extent), as compared with that of non-smokers (Figures 3E and S2D). This was also observed by a longitudinal analysis comparing smoker controls and non-smokers, with this upregulation persisting in long-term cultures (Figure 3E). When assessing the potential effect of (active) smoking on the expression pattern, *SPDEF* expression was decreased in smokers who quit smoking for more than 4 years as compared with active smokers and ex-smokers with a smoking cessation of less than 4 years, in early, short-term, mid-term and to long-term cultures (Figure 3F and S2E). Similarly, longitudinal analysis showed that *FOXA3* was also upregulated in smoker controls as compared with non-smokers and mild and moderate COPD (Figure S2F), and that it was decreased in smokers who quit smoking for more than 4 years (Figure 3G and S2G). These data show that goblet cell hyperplasia relates to smoking and demonstrate that this feature persists over time *in vitro*.

Epithelial-to-mesenchymal transition of the COPD AE

The expression of EMT protein markers (vimentin, fibronectin) was assessed in long-term ALI cultures. Increased vimentin content was observed in early, short-term and mid-term cultures, but no more in long-term cultures of (very) severe COPD AE as compared with non-smoker controls (Figure 4A-B), as well as in smokers and mild/moderate COPD AE in early ALI-AE. Accordingly, mild/moderate and (very) severe COPD AE displayed increased fibronectin release in the basolateral medium up to mid-term cultures, as compared with non-smokers, while it was significantly increased only in early ALI-AE from control smokers (Figure 4C). No difference was seen anymore in long-term cultures. No striking difference was seen regarding vimentin mRNA abundance (*VIM*, Figure S3). These data show EMT features are slowly but progressively vanishing in COPD, and even more rapidly in smokers, as summarized in Figure 4D.

Polarity and pIgR/SC expression in the COPD vs control AE

Smokers- and COPD-derived AE released less apical SC than non-smokers, from short-term up to long-term ALI cultures (Figure 5A), a decrease that correlates with disease severity (Figure 5B and S4A). When analyzed longitudinally over 10 weeks, this decrease was more pronounced in (very) severe COPD as compared with smoker controls and mild/moderate COPD (Figure 5C). Similarly, the (very) severe COPD AE displayed decreased *PIGR* mRNA abundance throughout the long-term cultures as compared with the other groups. Although this was not significant on isolated time points (Figure 5D and S4B), longitudinal data analysis demonstrated decreased *PIGR* mRNA abundance in (very) severe COPD AE as compared with non-smokers, smoker controls, and mild/moderate COPD AE (Figure 5D). In addition, considering that epithelial differentiation is completed at 5 weeks, we show that the acquisition of optimal pIgR protein levels was delayed in COPD AEs compared with controls, as depicted in Figure 5E, where representative blots of pIgR expression kinetics (1-5 weeks) in non-smoker (upper gel) and very severe COPD (lower gel) ALI-AE are represented.

These data show that airway epithelial polarity, witnessed by the pIgR/SC expression, is deeply impaired in COPD in a persistent manner.

Inflammatory cytokine production by the COPD vs control AE

Epithelial production of IL-8/CXCL-8 and IL-6 was next assayed in the reconstituted AE. A trend for increased *CXCL8* mRNA abundance was seen in smokers and COPD groups, that was more marked in early to mid-term ALI culture (Figure S5A). Accordingly, IL-8/CXCL-8 release was strongly increased in early, short-term and mid-term AE from smokers- and COPD-derived as compared with that of non-smokers, whilst this difference disappeared afterwards (Figure 6A). Although no difference was observed regarding *IL6* mRNA abundance (Figure S5B), the IL-6 production in the basolateral medium was increased in smokers and COPD ALI-AE. In contrast to IL-8, IL-6 upregulation persisted over time (up to long-term cultures), both in smokers and COPD (Figures 6B).

Exogenous inflammation induces COPD-like features in the AE

Next, we assessed whether exogenous inflammation could promote COPD-like changes in the AE by supplementing the culture medium with IL-6, TNF-α and IL-1β (all at 5ng/ml) for 5 weeks. These cytokines are relevant to human COPD pathogenesis, as besides the abovementioned CXCL-8/IL-8 and IL-6, TNF-α and IL-1β are also increased in COPD (26, 43), even though their concentration did not reach the detection threshold in our culture supernatants (not shown).

First, TEER was dramatically decreased upon exposure to the inflammatory stimuli. This was already observed in early cultures but was more pronounced in the subsequent weeks (Figure 7A). Cytokine-exposed cultures displayed similar values irrespectively of the original phenotype, with TEER values comprised between 300 and 600 Ω/cm² in early and mid-term

cultures, possibly indicating a maximal effect on barrier (dys)function at the used concentrations.

Second, cultures that were exposed to inflammatory cytokines displayed sharper EMT features, with increased fibronectin release in early, short-term and mid-term cultures (Figure 7B). Interestingly, this induction that was not observed in non-smokers' AE, was strikingly upregulated in COPD as compared to (non-)smoker controls (Figure 7C). Congruently, similar results could be observed when assessing vimentin expression (Figure 7D). These results show that the cultured AE from COPD patients, whilst losing its intrinsic EMT features, remains prone to develop EMT upon exposure to inflammatory cytokines.

Third, cytokine-induced inflammation altered epithelial polarity assayed through the pIgR/SC system, as SC apical release was decreased in cytokine-exposed AE from non-smoker controls, smoker controls and mild-to-moderate COPD (Figure 7E). This was not observed in (very) severe COPD AE, probably because the pIgR/SC system is already severely impaired in this group.

In conclusion, exogenous inflammation was able to induce COPD-like changes such as barrier dysfunction, EMT and altered polarity in the AE from non-smoker and smoker controls. In addition, the COPD-derived AE remained prone to develop EMT features upon inflammatory stimulation.

Epithelial progenitors as keepers of the memory of epithelial damage in COPD

Basal cells and club cells constitute progenitor cells of the airway epithelium, with the latter being restricted to small airways (44). In COPD, recent data unanimously depict impaired basal cells functionality in terms of differentiation, signalling and transcriptome (18, 45-47), while little is known about club cells progenitor (dys)function in COPD. Using a scRNAseq database assessing distal lung cell populations from non-smokers, non-COPD smokers and COPD

patients (courtesy of Pr. Yamamoto, National Cancer Center Research Institute, Tokyo, Japan; preprint available at reference (39)), airway progenitor populations (both basal and club cells, Figure 8A-B) were selectively explored for the transcription of EMT-related genes in COPD, as compared with non-smokers and non-COPD smokers. We show that *VIM*, *FN1*, *SNAI1*, *SNAI2*, *S100A2*, and *S100A4* mRNA abundance was increased in basal and club cells from COPD patients, as compared with controls (pooled non-smokers and non-COPD smokers), suggesting EMT reprogramming of these cells (Figure 8C-H). However, this increase does not reach statistical significance, due to two main factors: first, stringent false discovery rate correction has been applied, as more than 10.000 genes have been studied in the original study; second, low basal and club cell counts were observed in those distal (and mostly parenchymal) samples.

Discussion

This study demonstrates, by exploiting long-term cultures of the ALI-reconstituted human AE from well-characterized COPD and control patients, that the AE retains its native abnormalities for prolonged periods of time (e.g. barrier dysfunction, altered cell differentiation, and impaired polarity) whereas some features (IL-8 upregulation, EMT) disappear. It also demonstrates that inflammation, driven by TNF-α, IL-6 and IL-1β, may induce a COPD-like phenotype and reactivates EMT programming in the diseased (COPD) epithelium. Single-cell RNAseq data suggest that the mechanisms underlying the persistence of COPD-related airway epithelium alterations lay in progenitor cells.

COPD is a chronic and progressive disease that is developed upon repeated injury of the airway epithelial-mesenchymal unit by toxics, leading to activation and remodeling of the AE, and ultimately to irreversible airway obstruction. It has been shown that COPD patients who quit smoking may benefit from decreases in mortality (31), respiratory symptoms and lung function decline as compared with active smokers (30, 48, 49). They also display reduced AE

remodeling and goblet cell hyperplasia when smoking cessation exceeds 3.5 years (29), as well as improvements in nasal mucociliary clearance (50). In contrast, no change was observed following smoking cessation regarding axonemal abnormalities in ciliated cells (51), airway mucosal inflammation (33), sputum IL-8/CXCL-8 (52) or sputum neutrophils (32, 52), potentially suggesting permanent alterations in these compartments.

In this study, we assessed whether the irreversible nature of the disease is imprinted in the AE in such a way that aberrant features of the native epithelium persist in long-term cultures, independently of signals provided by repeated insults and/or by mesenchymal cells and surrounding leukocytes. The ALI model was used, as it was previously shown to recapitulate, at least to some extent, the native COPD phenotype (8, 10, 17, 18, 53). We prolonged the culture up to 10 weeks, an unusually long duration in this model, that had not yet been reported so far in COPD.

A major abnormality that persists in the cultured smokers' and COPD AE is the barrier and junctional defect (7). Thus, the AE from smokers displays a persistent TEER decrease as compared with that from non-smokers, which was associated with decreased protein levels of E-cadherin and occludin, key components of adherens and tight junctions, respectively. This observation is in line with a previous study showing that CS exposure leads to disruption of apical junctional complexes (54). We here show that this alteration further persists in long-term cultures for occludin. In addition, those changes in TEER and E-cadherin/occludin expression were further downregulated according to the presence and severity of COPD. Meanwhile, mRNA abundance for the main apical junctional complexes' components (*TJP1*, *OCLN*, *ECAD*, *CLDN11*, Figure S1) did not differ across the groups, suggesting an effect of post-transcriptional regulation.

In line with the requirement of the integrity of apical junctional complexes to ensure baso-apical epithelial polarity (55), our study shows that AE polarity is persistently impaired in COPD. The

pIgR/SC system, that allows baso-apical transcytosis of polymeric immunoglobulins (mostly dimeric IgA) across the epithelium and constitutes a marker of epithelial polarity (19), was previously shown to be defective in COPD, both *in situ* in surgical tissue and *in vitro* in ALI-HBEC evaluated at 2 weeks cultures (17). The present study demonstrates that this impairment persists over time, with decreases in the apical release of SC and in the mRNA abundance of *PIGR*, observed in very severe COPD (Figures 5 and S4). In addition, the dynamics of optimal pIgR protein expression, were delayed in COPD AE (Figure 5D). Interestingly, those data are contrasting with previous findings in asthma where pIgR downregulation, although being similarly present *in situ*, does not persist in ALI cultures from asthma patients (56), suggesting distinct mechanisms driving epithelial pathology in asthma and COPD.

Aside from these findings, our study demonstrates that ciliated cell hypoplasia – with decreased *FOXJ1* and *DNAI1* mRNA abundance – also persists in long-term ALI cultures from COPD patients. In addition, it shows that goblet cell hyperplasia persists in smokers, as witnessed by *SPDEF* upregulation which remains higher in active smokers and ex-smokers who quit for less than 4 years, as compared with ex-smokers who quit for more than 4 years (Figures 3F and S2D). These results corroborate previous findings indicating that this secretory trait relates more directly to smoking rather than to the disease (29).

In contrast with those changes, some abnormalities are observed only in short-term culture, such as EMT. EMT is a dynamic process where cells lose their epithelial features and gain mesenchymal properties, including migratory abilities, which is required for normal embryogenesis (type I EMT), tissue repair (type II), or cancer metastasis (type III). In COPD, airway fibrosis probably follows persistent type II EMT (57). ALI-AE from COPD patients spontaneously exhibit mesenchymal features, and CS may induce EMT in control HBEC (14), possibly as a result of TGF-β signalling (8). Accordingly, our results show EMT features (vimentin expression, fibronectin release) overexpression in the AE from control smokers and

COPD patients during the first weeks of culture. However, these features further vanish from mid-term cultures onwards, with complete disappearance occurring earlier in smoker controls than in COPD samples. Moreover, we highlight that, even though EMT markers are vanishing, the COPD AE remains prone to reactivate EMT programming upon inflammatory condition, suggesting the existence of a priming state in the COPD AE, imprinted by previous (*in vivo*) exposures conditioning its responses to further stimulation. As a dedicated analysis of airway progenitor cells transcriptome, issued from a scRNAseq database from distal lung samples (39) shows that EMT-related genes are upregulated *in situ* in basal and club cells from COPD patients, we suggest that this priming state resides in these cell types.

As observed for EMT, upregulation of IL-8/CXCL-8 release by the smokers' and COPD AE is also fading away from mid-term cultures onwards. In contrast, IL-6 overproduction persisted in long term ALI-AE from both control smokers and COPD patients. Finally, *in vitro* exposure to inflammatory cytokines reproduced or aggravated alterations in barrier and polarity features as well as EMT in controls and COPD AE, respectively.

The fundamental mechanisms of these observations question the nature of epithelial memory. Inflammatory memory refers to memories of previous immune events enabling barrier tissues to rapidly recall distinct environmental exposures, which may be stored not only in immune cells but also in epithelial and mesenchymal cells (58, 59). While memory classically refers in the immune system to somatic mutations underlying adaptive antibody responses to recall antigens, "inflammatory memory" is less well defined and may include epigenetic modifications and chromatin changes that may drive persistent changes in damaged tissues. It was proposed that the memory distribution could promote maladaptation in disease, particularly if cellular cooperation is potentiated (i.e. collective memory owing to different cell types) during recall responses. Progenitor basal cells are prime candidates to retain epithelial memory in the airways, as do epithelial progenitors in the skin towards inflammatory or mechanical

stress by maintaining accessibility of key stress response genes through chromatin modifications (59) as well as in the gut towards dietary components (60). Interestingly, WNT signalling, which is upregulated in the COPD AE (18), has been shown to be involved in the latter form of epithelial memory abd may regulate stemness and tumorigenicity. In line with the recent hypothesis that basal cells serve as repositories of allergic inflammatory memory in respiratory epithelial cells (58), and based on the differences observed in EMT-related genes in COPD basal cells, one could propose that airway stem cells (basal cells, and club cells in small airways) also store the memory of repeated previous injuries by inhaled toxics such as cigarette smoke.

Our study has several limitations. First, an effect of treatments (especially inhaled corticosteroids in severe patients) on the findings cannot be excluded. However, *in vitro* studies on intestinal cell lines and primary human bronchial and nasal epithelial cells in ALI culture showed dexamethasone-induced increases in TEER, claudin-2 (61), and E-cadherin (62, 63) expression, while budesonide exposure of ALI-HBEC counter-acted CS-induced barrier dysfunction (64). In addition, dexamethasone and fluticasone propionate improved TGF-β_1-induced EMT in A549 cells and in primary airway nasal cells (65), suggesting that corticosteroids may rather improve barrier function and EMT changes. Second, the imprinting observed in this model of *ex vivo* reconstituted epithelium, which involves (following proliferation and differentiation of basal cells) prolonged culture of slowly-to-non-dividing cells, should be confirmed in other models such as airway organoids and culture following multiple passages.

In conclusion, this study demonstrates that the AE from smokers and COPD stores the memory of its native state and previous insults from cigarette smoking, in addition to additional signals that underlie the development of the disease itself. This memory is multidimensional, including alterations in barrier function, epithelial polarity, and lineage differentiation, as well as IL-6

release and EMT reprogramming. In line with other studies and based on scRNAseq data in basal and club cells, we suggest that the COPD-related memory is imprinted in progenitor cells which contribute to the persistence of disease by serving as repositories for toxic inflammatory memories in the airways.

References

1. Organization WH. Chronic respiratory diseases. 2017 [Available from: http://www.who.int/respiratory/copd/burden/en/.

2. Salvi SS, Barnes PJ. Chronic obstructive pulmonary disease in non-smokers. Lancet. 2009;374(9691):733-43.

3. McDonough JE, Yuan R, Suzuki M, Seyednejad N, Elliott WM, Sanchez PG, et al. Small-airway obstruction and emphysema in chronic obstructive pulmonary disease. N Engl J Med. 2011;365(17):1567-75.

4. Vogelmeier CF, Criner GJ, Martinez FJ, Anzueto A, Barnes PJ, Bourbeau J, et al. Global Strategy for the Diagnosis, Management, and Prevention of Chronic Obstructive Lung Disease 2017 Report. GOLD Executive Summary. Am J Respir Crit Care Med. 2017;195(5):557-82.

5. Celli BR, Anderson JA, Cowans NJ, Crim C, Hartley BF, Martinez FJ, et al. Pharmacotherapy and Lung Function Decline in Patients with Chronic Obstructive Pulmonary Disease: A Systematic Review. Am J Respir Crit Care Med. 2020.

6. Aghapour M, Raee P, Moghaddam SJ, Hiemstra PS, Heijink IH. Airway Epithelial Barrier Dysfunction in Chronic Obstructive Pulmonary Disease: Role of Cigarette Smoke Exposure. Am J Respir Cell Mol Biol. 2018;58(2):157-69.

7. Carlier FM, de Fays C, Pilette C. Epithelial Barrier Dysfunction in Chronic Respiratory Diseases. Frontiers in Physiology. 2021;12(861).

8. Gohy ST, Hupin C, Fregimilicka C, Detry BR, Bouzin C, Gaide Chevronay H, et al. Imprinting of the COPD airway epithelium for dedifferentiation and mesenchymal transition. Eur Respir J. 2015;45(5):1258-72.

9. Yaghi A, Dolovich MB. Airway Epithelial Cell Cilia and Obstructive Lung Disease. Cells. 2016;5(4).

10. Gohy S, Carlier FM, Fregimilicka C, Detry B, Lecocq M, Ladjemi MZ, et al. Altered generation of ciliated cells in chronic obstructive pulmonary disease. Sci Rep. 2019;9(1):17963.

11. Pilette C, Godding V, Kiss R, Delos M, Verbeken E, Decaestecker C, et al. Reduced epithelial expression of secretory component in small airways correlates with airflow obstruction in chronic obstructive pulmonary disease. Am J Respir Crit Care Med. 2001;163(1):185-94.

12. Gamez AS, Gras D, Petit A, Knabe L, Molinari N, Vachier I, et al. Supplementing defect in club cell secretory protein attenuates airway inflammation in COPD. Chest. 2015;147(6):1467-76.

13. Saetta M, Turato G, Baraldo S, Zanin A, Braccioni F, Mapp CE, et al. Goblet cell hyperplasia and epithelial inflammation in peripheral airways of smokers with both symptoms of chronic bronchitis and chronic airflow limitation. Am J Respir Crit Care Med. 2000;161(3 Pt 1):1016-21.

14. Milara J, Peiro T, Serrano A, Cortijo J. Epithelial to mesenchymal transition is increased in patients with COPD and induced by cigarette smoke. Thorax. 2013;68(5):410-20.

15. Mahmood MQ, Sohal SS, Shukla SD, Ward C, Hardikar A, Noor WD, et al. Epithelial mesenchymal transition in smokers: large versus small airways and relation to airflow obstruction. Int J Chron Obstruct Pulmon Dis. 2015;10:1515-24.

16. Sohal SS. Chronic Obstructive Pulmonary Disease (COPD) and Lung Cancer: Epithelial Mesenchymal Transition (EMT), the Missing Link? EBioMedicine. 2015;2(11):1578-9.

17. Gohy ST, Detry BR, Lecocq M, Bouzin C, Weynand BA, Amatngalim GD, et al. Polymeric immunoglobulin receptor down-regulation in chronic obstructive pulmonary disease. Persistence in the cultured epithelium and role of transforming growth factor-beta. Am J Respir Crit Care Med. 2014;190(5):509-21.

18. Carlier FM, Dupasquier S, Ambroise J, Detry B, Lecocq M, Bietry-Claudet C, et al. Canonical WNT pathway is activated in the airway epithelium in chronic obstructive pulmonary disease. EBioMedicine. 2020;61:103034.

19. Carlier FM, Sibille Y, Pilette C. The epithelial barrier and immunoglobulin A system in allergy. Clin Exp Allergy. 2016;46(11):1372-88.

20. Pilette C, Ouadrhiri Y, Godding V, Vaerman JP, Sibille Y. Lung mucosal immunity: immunoglobulin-A revisited. Eur Respir J. 2001;18(3):571-88.

21. Pilette C, Durham SR, Vaerman JP, Sibille Y. Mucosal immunity in asthma and chronic obstructive pulmonary disease: a role for immunoglobulin A? Proc Am Thorac Soc. 2004;1(2):125-35.

22. Polosukhin VV, Richmond BW, Du RH, Cates JM, Wu P, Nian H, et al. Secretory IgA Deficiency in Individual Small Airways Is Associated with Persistent Inflammation and Remodeling. Am J Respir Crit Care Med. 2017;195(8):1010-21.

23. Polosukhin VV, Cates JM, Lawson WE, Zaynagetdinov R, Milstone AP, Massion PP, et al. Bronchial secretory immunoglobulin a deficiency correlates with airway inflammation and progression of chronic obstructive pulmonary disease. Am J Respir Crit Care Med. 2011;184(3):317-27.

24. Barnes PJ. Inflammatory mechanisms in patients with chronic obstructive pulmonary disease. J Allergy Clin Immunol. 2016;138(1):16-27.

25. Eapen MS, Myers S, Walters EH, Sohal SS. Airway inflammation in chronic obstructive pulmonary disease (COPD): a true paradox. Expert Rev Respir Med. 2017;11(10):827-39.

26. Keatings VM, Collins PD, Scott DM, Barnes PJ. Differences in interleukin-8 and tumor necrosis factor-alpha in induced sputum from patients with chronic obstructive pulmonary disease or asthma. Am J Respir Crit Care Med. 1996;153(2):530-4.

27. Rutgers SR, Timens W, Kaufmann HF, van der Mark TW, Koeter GH, Postma DS. Comparison of induced sputum with bronchial wash, bronchoalveolar lavage and bronchial biopsies in COPD. Eur Respir J. 2000;15(1):109-15.

28. Di Stefano A, Capelli A, Lusuardi M, Balbo P, Vecchio C, Maestrelli P, et al. Severity of airflow limitation is associated with severity of airway inflammation in smokers. Am J Respir Crit Care Med. 1998;158(4):1277-85.

29. Lapperre TS, Sont JK, van Schadewijk A, Gosman MM, Postma DS, Bajema IM, et al. Smoking cessation and bronchial epithelial remodelling in COPD: a cross-sectional study. Respir Res. 2007;8:85.

30. Willemse BW, Postma DS, Timens W, ten Hacken NH. The impact of smoking cessation on respiratory symptoms, lung function, airway hyperresponsiveness and inflammation. Eur Respir J. 2004;23(3):464-76.

31. Bai JW, Chen XX, Liu S, Yu L, Xu JF. Smoking cessation affects the natural history of COPD. Int J Chron Obstruct Pulmon Dis. 2017;12:3323-8.

32. Louhelainen N, Rytila P, Haahtela T, Kinnula VL, Djukanovic R. Persistence of oxidant and protease burden in the airways after smoking cessation. BMC Pulm Med. 2009;9:25.

33. Gamble E, Grootendorst DC, Hattotuwa K, O'Shaughnessy T, Ram FS, Qiu Y, et al. Airway mucosal inflammation in COPD is similar in smokers and ex-smokers: a pooled analysis. Eur Respir J. 2007;30(3):467-71.

34. Lapperre TS, Postma DS, Gosman MM, Snoeck-Stroband JB, ten Hacken NH, Hiemstra PS, et al. Relation between duration of smoking cessation and bronchial inflammation in COPD. Thorax. 2006;61(2):115-21.

35. Pauwels RA, Buist AS, Ma P, Jenkins CR, Hurd SS, Committee GS. Global strategy for the diagnosis, management, and prevention of chronic obstructive pulmonary disease: National Heart, Lung, and Blood Institute and World Health Organization Global Initiative for Chronic Obstructive Lung Disease (GOLD): executive summary. Respir Care. 2001;46(8):798-825.

36. Bustin SA, Benes V, Garson J, Hellemans J, Huggett J, Kubista M, et al. The need for transparency and good practices in the qPCR literature. Nat Methods. 2013;10(11):1063-7.

37. Pilette C, Ouadrhiri Y, Dimanche F, Vaerman JP, Sibille Y. Secretory component is cleaved by neutrophil serine proteinases but its epithelial production is increased by neutrophils through NF-kappa B- and p38 mitogen-activated protein kinase-dependent mechanisms. Am J Respir Cell Mol Biol. 2003;28(4):485-98.

38. Collin AM, Lecocq M, Noel S, Detry B, Carlier FM, Aboubakar Nana F, et al. Lung immunoglobulin A immunity dysregulation in cystic fibrosis. EBioMedicine. 2020;60:102974.

39. Watanabe N, Nakayama J, Fujita Y, Mori Y, Kadota T, Shimomura I, et al. Single-cell Transcriptome Analysis Reveals an Anomalous Epithelial Variation and Ectopic Inflammatory Response in Chronic Obstructive Pulmonary Disease. medRxiv. 2020:2020.12.03.20242412.

40. Chen G, Korfhagen TR, Karp CL, Impey S, Xu Y, Randell SH, et al. Foxa3 induces goblet cell metaplasia and inhibits innate antiviral immunity. Am J Respir Crit Care Med. 2014;189(3):301-13.

41. Park KS, Korfhagen TR, Bruno MD, Kitzmiller JA, Wan H, Wert SE, et al. SPDEF regulates goblet cell hyperplasia in the airway epithelium. J Clin Invest. 2007;117(4):978-88.

42. Rajavelu P, Chen G, Xu Y, Kitzmiller JA, Korfhagen TR, Whitsett JA. Airway epithelial SPDEF integrates goblet cell differentiation and pulmonary Th2 inflammation. J Clin Invest. 2015;125(5):2021-31.

43. Bafadhel M, McKenna S, Terry S, Mistry V, Reid C, Haldar P, et al. Acute exacerbations of chronic obstructive pulmonary disease: identification of biologic clusters and their biomarkers. Am J Respir Crit Care Med. 2011;184(6):662-71.

44. Rawlins EL, Okubo T, Xue Y, Brass DM, Auten RL, Hasegawa H, et al. The role of Scgb1a1+ Clara cells in the long-term maintenance and repair of lung airway, but not alveolar, epithelium. Cell Stem Cell. 2009;4(6):525-34.

45. Rock JR, Randell SH, Hogan BL. Airway basal stem cells: a perspective on their roles in epithelial homeostasis and remodeling. Dis Model Mech. 2010;3(9-10):545-56.

46. Ryan DM, Vincent TL, Salit J, Walters MS, Agosto-Perez F, Shaykhiev R, et al. Smoking dysregulates the human airway basal cell transcriptome at COPD risk locus 19q13.2. PLoS One. 2014;9(2):e88051.

47. Zuo WL, Yang J, Gomi K, Chao I, Crystal RG, Shaykhiev R. EGF-Amphiregulin Interplay in Airway Stem/Progenitor Cells Links the Pathogenesis of Smoking-induced Lesions in the Human Airway Epithelium. Stem Cells. 2016.

48. Anthonisen NR, Connett JE, Kiley JP, Altose MD, Bailey WC, Buist AS, et al. Effects of smoking intervention and the use of an inhaled anticholinergic bronchodilator on the rate of decline of FEV1. The Lung Health Study. JAMA. 1994;272(19):1497-505.

49. Fletcher C, Peto R. The natural history of chronic airflow obstruction. Br Med J. 1977;1(6077):1645-8.

50. Ramos EM, De Toledo AC, Xavier RF, Fosco LC, Vieira RP, Ramos D, et al. Reversibility of impaired nasal mucociliary clearance in smokers following a smoking cessation programme. Respirology. 2011;16(5):849-55.

51. Verra F, Escudier E, Lebargy F, Bernaudin JF, De Cremoux H, Bignon J. Ciliary abnormalities in bronchial epithelium of smokers, ex-smokers, and nonsmokers. Am J Respir Crit Care Med. 1995;151(3 Pt 1):630-4.

52. Willemse BW, ten Hacken NH, Rutgers B, Lesman-Leegte IG, Postma DS, Timens W. Effect of 1-year smoking cessation on airway inflammation in COPD and asymptomatic smokers. Eur Respir J. 2005;26(5):835-45.

53. Carlier F, Detry B, Sibille Y, Pilette C. COPD epithelial phenotype shows partial reversibility in long-term primary epithelial ALI-cultures. Eur Respir J. 2018;52(suppl 62).

54. Shaykhiev R, Otaki F, Bonsu P, Dang DT, Teater M, Strulovici-Barel Y, et al. Cigarette smoking reprograms apical junctional complex molecular architecture in the human airway epithelium in vivo. Cell Mol Life Sci. 2011;68(5):877-92.

55. Cereijido M, Valdes J, Shoshani L, Contreras RG. Role of tight junctions in establishing and maintaining cell polarity. Annu Rev Physiol. 1998;60:161-77.

56. Ladjemi MZ, Gras D, Dupasquier S, Detry B, Lecocq M, Garulli C, et al. Bronchial Epithelial IgA Secretion Is Impaired in Asthma. Role of IL-4/IL-13. Am J Respir Crit Care Med. 2018;197(11):1396-409.

57. Bartis D, Mise N, Mahida RY, Eickelberg O, Thickett DR. Epithelial-mesenchymal transition in lung development and disease: does it exist and is it important? Thorax. 2014;69(8):760-5.

58. Ordovas-Montanes J, Beyaz S, Rakoff-Nahoum S, Shalek AK. Distribution and storage of inflammatory memory in barrier tissues. Nat Rev Immunol. 2020;20(5):308-20.

59. Naik S, Larsen SB, Gomez NC, Alaverdyan K, Sendoel A, Yuan S, et al. Inflammatory memory sensitizes skin epithelial stem cells to tissue damage. Nature. 2017;550(7677):475-80.

60. Beyaz S, Mana MD, Roper J, Kedrin D, Saadatpour A, Hong SJ, et al. High-fat diet enhances stemness and tumorigenicity of intestinal progenitors. Nature. 2016;531(7592):53-8.

61. Fischer A, Gluth M, Weege F, Pape UF, Wiedenmann B, Baumgart DC, et al. Glucocorticoids regulate barrier function and claudin expression in intestinal epithelial cells via MKP-1. Am J Physiol Gastrointest Liver Physiol. 2014;306(3):G218-28.

62. Carayol N, Vachier I, Campbell A, Crampette L, Bousquet J, Godard P, et al. Regulation of E-cadherin expression by dexamethasone and tumour necrosis factor-alpha in nasal epithelium. Eur Respir J. 2002;20(6):1430-6.

63. Carayol N, Campbell A, Vachier I, Mainprice B, Bousquet J, Godard P, et al. Modulation of cadherin and catenins expression by tumor necrosis factor-alpha and dexamethasone in human bronchial epithelial cells. Am J Respir Cell Mol Biol. 2002;26(3):341-7.

64. Heijink I, van den Berge M, Kliphuis N, ten Hacken N, Postma D, van Oosterhout A. Corticosteroids improve airway epithelial regeneration and restore oxidative stress-induced epithelial barrier dysfunction. Eur Respir J. 2012;40(Suppl 56).

65. Yang HW, Lee SA, Shin JM, Park IH, Lee HM. Glucocorticoids ameliorate TGF-beta1-mediated epithelial-to-mesenchymal transition of airway epithelium through MAPK and Snail/Slug signaling pathways. Sci Rep. 2017;7(1):3486.

Tables

	Non-smoker controls (n=10)	Smoker controls (n=15)	COPD 1-2 (n=13)	COPD 3-4 (n=13)	
N (Male/Female)	10 (4/6)	15 (11/4)	13 (6/7)	13 (5/8)	ns
Age (y)	68.7 ± 13.2	64.2 ± 9.0	64.4 ± 9.5	59.8 ± 4.6	ns
Smoking history (never/former/current n)	10/0/0	0/10/5	0/4/9	0/13/0	p=0.001
Pack-years	0.0 ± 0	32.5 ± 20.7*	43.1 ± 19.6*	43.2 ± 23.1*	p<0.0001
If applicable, duration since smoking cessation (mo)	NA	154.0 ± 154.1	50.0 ± 55.5	90.6 ± 87.0	ns
FEV1 (% of PV)	104.8 ± 15.5	95.5 ± 14.7	74.1 ± 9.7*#	23.6 ± 6.1*#¶	p<0.0001
FEV1/VC ratio (%)	79.4 ± 6.9	78.5 ± 6.8	59.9 ± 9.3*#	33.2 ± 6.6*#¶	p<0.0001
DLCO (% of PV)	77.7 ± 13.0	69.9 ± 14.1	59.2 ± 19.1*	35.6 ± 8.0*#¶	p<0.0001
BMI ($kg.m^{-2}$)	27.8 ± 5.7	26.7 ± 5.2	25.4 ± 5.8	23.8 ± 4.0	ns
Inhaled corticosteroids (n/total N)	0/10	1/15	1/13	12/13	p<0.0001

Table 1 | Patient cohort for ALI-cultures. Data are presented as mean ± SD, unless otherwise stated. Demographic data, lung function tests, smoking history and inhaled corticotherapy are stated for the patient groups, classified according to smoking history and the presence and severity of airflow limitation. ALI, air/liquid interface; BMI, body mass index; COPD, chronic obstructive pulmonary disease; DLCO, diffusing capacity of the lung for CO; FEV1, forced expiratory volume in 1 s; mo, months; PV, predicted values; SD, standard deviation; VC, vital capacity; y, years.
* = p<0.05 compared to non-smoker controls
# = p<0.05 compared to smoker controls
¶ = p<0.05 compared to COPD stage 1-2 patients
ns, not significant

Figures

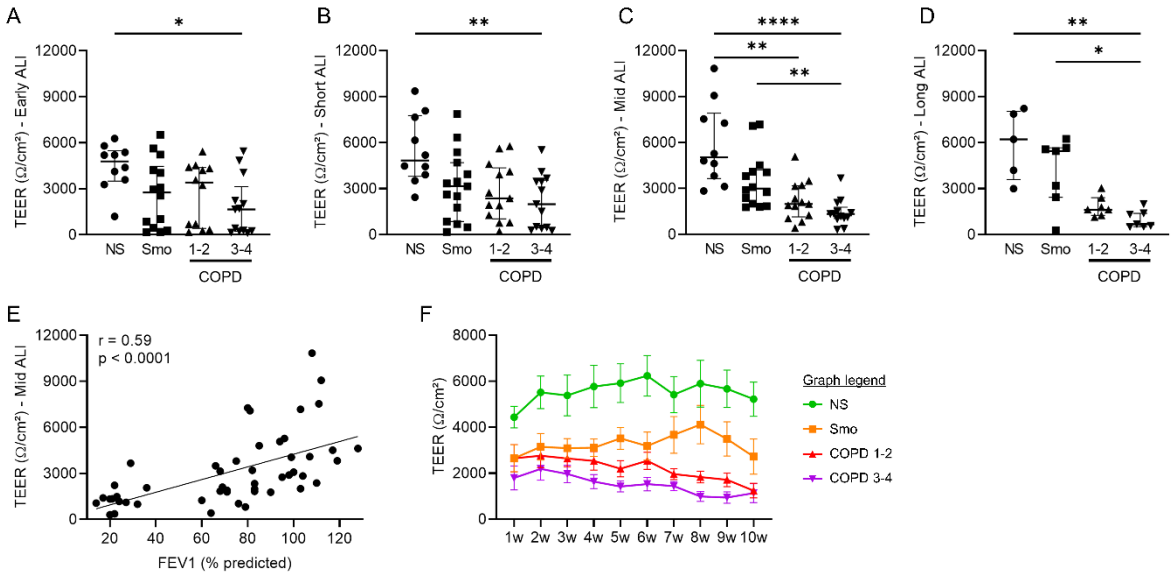

Figure 1 | COPD and smokers AE displays persistent decreased TEER compared with non-smokers AE.
A-D. TEER in the ALI-AE from non-smokers and smoker controls and COPD patients (GOLD classification from 1 to 4 according to the spirometric severity of the disease). Severe and very severe COPD AE show a sharp decrease in TEER as compared with (non)-smokers at all time periods, that is also observed to a lesser extent in mild and moderate COPD
E. The barrier dysfunction observed in COPD, witnessed by the TEER decrease, significantly correlates with the disease severity assessed by the FEV1. This is observed from short-term up to long-term cultures.
F. Longitudinal analysis of the evolution of the TEER in the ALI-AE from non-smokers, smoker controls, mild-to-moderate COPD and (very) severe COPD patients, showing a smoking-related persistent barrier dysfunction that is further enhanced in COPD. °, #, §, £ < 0.0001, $, ¶ < 0.001, mixed model analysis.
*, **, ***, **** indicate p-values of less than 0.05, 0.01, 0.001, and 0.0001, respectively (analysed using the Kruskal-Wallis test followed by Dunn's post-hoc test, except for H). Bars indicate median ± interquartile range, except for H, mean ± SEM. °: CT NS *versus* Smo; #: CT NS *versus* COPD 1-2, §: CT NS *versus* COPD 3-4, $: CT S *versus* COPD 1-2, £: CT S *versus* COPD 3-4, ¶: COPD 1-2 *versus* COPD 3-4
AE, airway epithelium; ALI, air-liquid interface; COPD, chronic obstructive pulmonary disease; FEV1, forced expired volume in 1 second; GAPDH, glyceralderhyde-3-phosphate dehydrogenase; NS, non-smokers; SEM, standard error of the mean; Smo, smokers; TEER, transepithelial electric resistance; w, weeks.

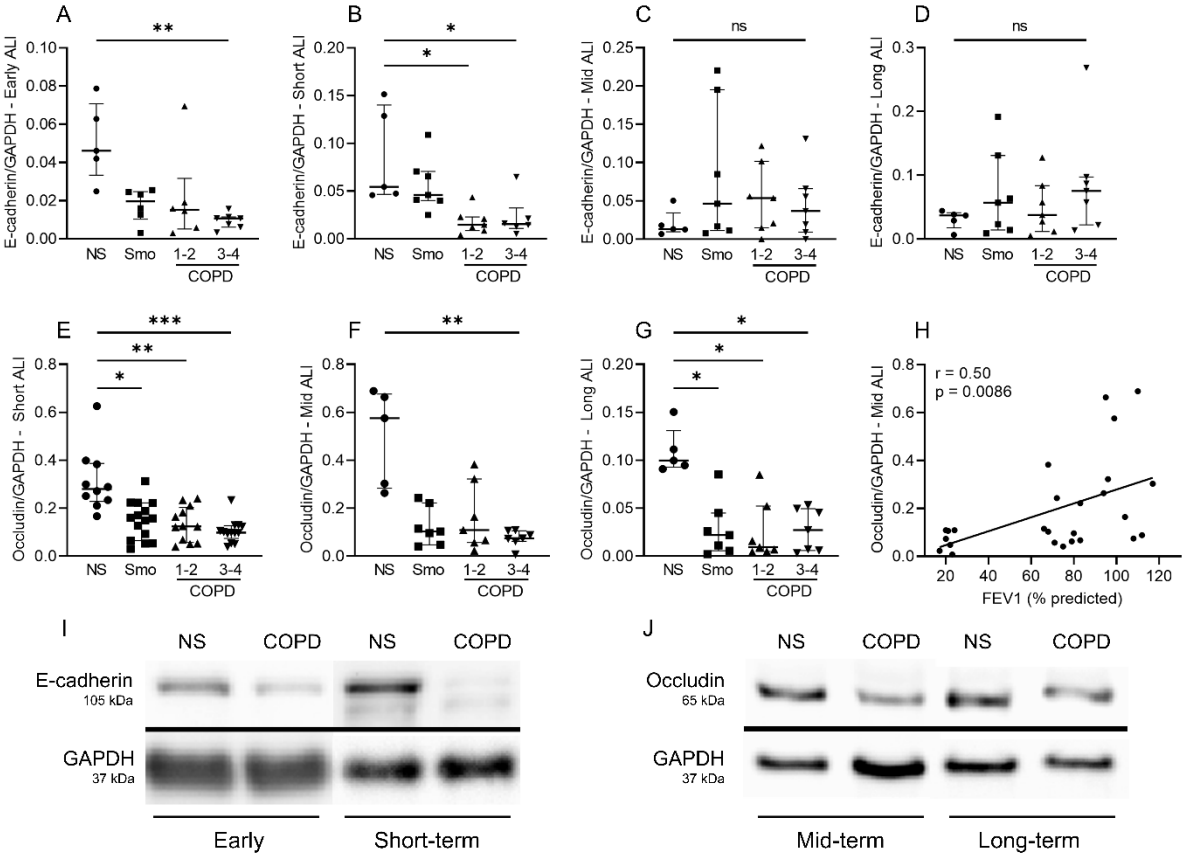

Figure 2 | COPD and smokers AE displays decreased E-cadherin and occludin protein expression compared with non-smokers AE.

A-D. Decreased E-cadherin protein levels in early and short-term ALI-AE, but no more at mid-term and long-term, in smoker controls and COPD ALI-AE as compared with that of non-smokers.

E-G. Decreased occludin protein levels, observable from short-term up to long-term cultures, in smoker controls and COPD ALI-AE as compared with that of non-smokers.

H. Occludin decrease in COPD AE significantly correlates with disease severity witnessed by the FEV1.

I. Representative blots for E-cadherin in non-smokers and very severe COPD AE, in early and short-term ALI-AE, showing decreased expression of E-cadherin at these time periods in COPD.

J. Representative blots for occludin in non-smokers and very severe COPD AE, in mid-term and long-term ALI-AE, showing decreased expression of occludin at these time periods in COPD.

*, **, *** indicate p-values of less than 0.05, 0.01, and 0.001, respectively (analysed using the Kruskal-Wallis test followed by Dunn's post-hoc test). Bars indicate median ± interquartile range.

AE, airway epithelium; ALI, air-liquid interface; COPD, chronic obstructive pulmonary disease; FEV1, forced expired volume in 1 second; NS, non-smokers; ns, not significant; SEM, standard error of the mean; Smo, smokers.

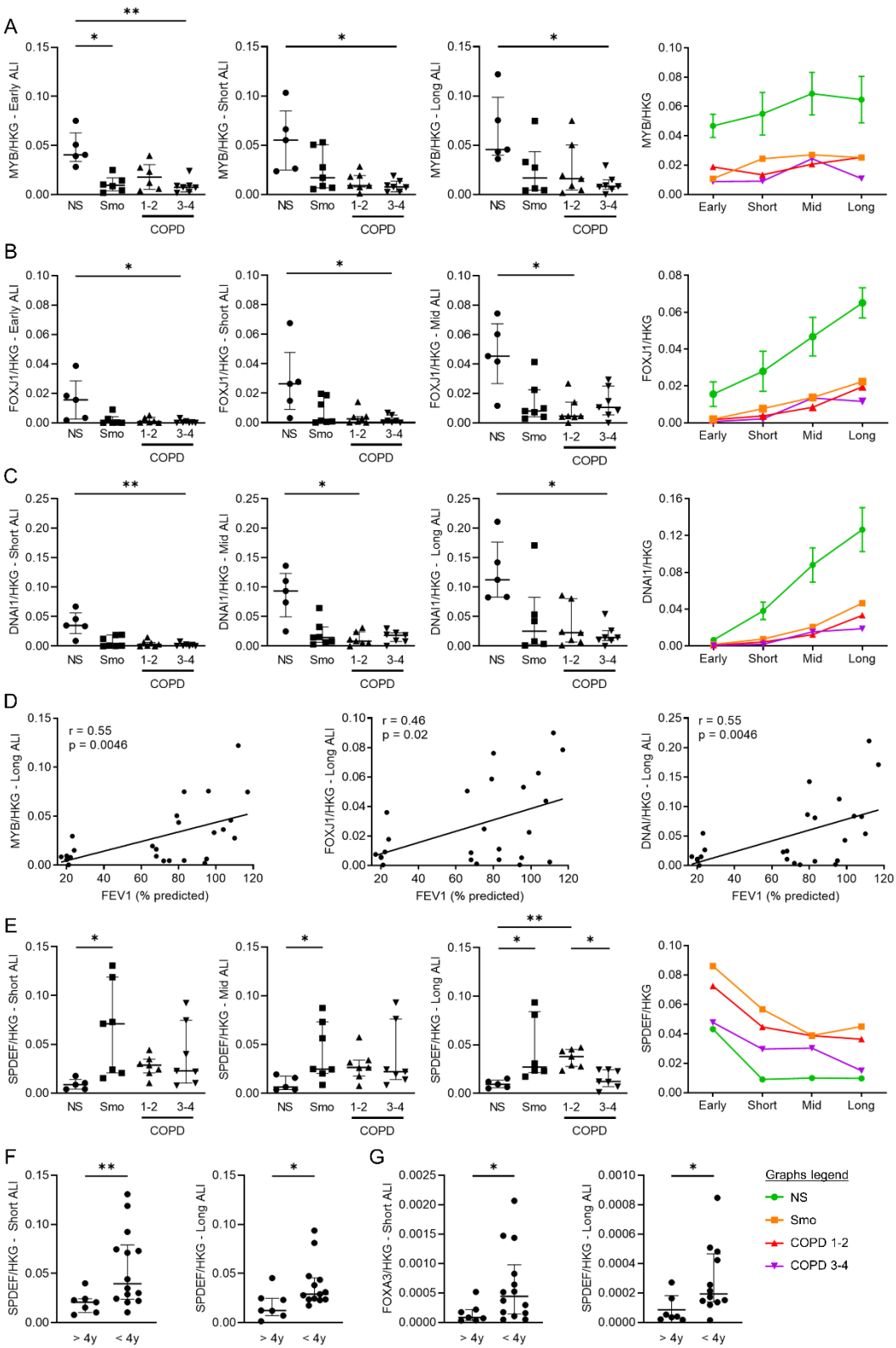

Figure 3 | Altered differentiation programming in smoker controls and COPD patients.

A. Decreased *MYB* expression in smokers and COPD AE, in early, short-term, and long-term ALI culture. Longitudinal analysis shows a strong, persistent down expression as compared with non-smokers. Right graph: $^{\#}$, § < 0.0001, ° < 0.001, $^{£}$ = 0.07, mixed model analysis.

B. Decreased *FOXJ1* expression in smokers and COPD AE, in early, short-term, and mid-term ALI culture. Longitudinal analysis shows a strong, persistent down expression as compared with non-smokers. Right graph: $^{\#}$, § < 0.0001, ° < 0.001, mixed model analysis.
C. Decreased *DNAI1* expression in smokers and COPD AE, in short-term, mid-term and long-term ALI culture. Longitudinal analysis shows a strong, persistent down expression as compared with non-smokers. Right graph: $^{\#}$, §, ° < 0.0001, mixed model analysis.
D. *MYB*, *FOXJ1*, and *DNAI1* downregulation in COPD patients correlates moderately with the disease severity, assessed by the FEV1.
E. Increased *SPDEF* expression in smokers AE as compared with non-smokers in short-term, mid-term and long-term ALI culture. Moreover, complementary longitudinal analysis shows increased expression in smokers as compared with COPD. Right graph: $^{\#}$, § < 0.01, $^{£}$ < 0.05, mixed model analysis.
F. *SPDEF* expression is decreased in smokers who quit smoking for more than 4 years.
G. *FOXA3* expression is decreased in smokers who quit smoking for more than 4 years.
*, **, ***, **** indicate p-values of less than 0.05, 0.01, 0.001, and 0.0001, respectively (analysed using the Kruskal-Wallis test followed by Dunn's post-hoc test, except for longitudinal data, mixed model). Bars indicate median ± interquartile range, except for longitudinal analysis, mean ± SEM. °: CT NS *versus* Smo; $^{\#}$: CT NS *versus* COPD 1-2, §: CT NS *versus* COPD 3-4, $^{£}$: CT S *versus* COPD 3-4.
AE, airway epithelium; ALI, air-liquid interface; COPD, chronic obstructive pulmonary disease; CT, control; FEV1, forced expired volume in 1 second; HKG, housekeeping genes; NS, non-smokers; SEM, standard error of the mean; Smo, smokers; y, years.

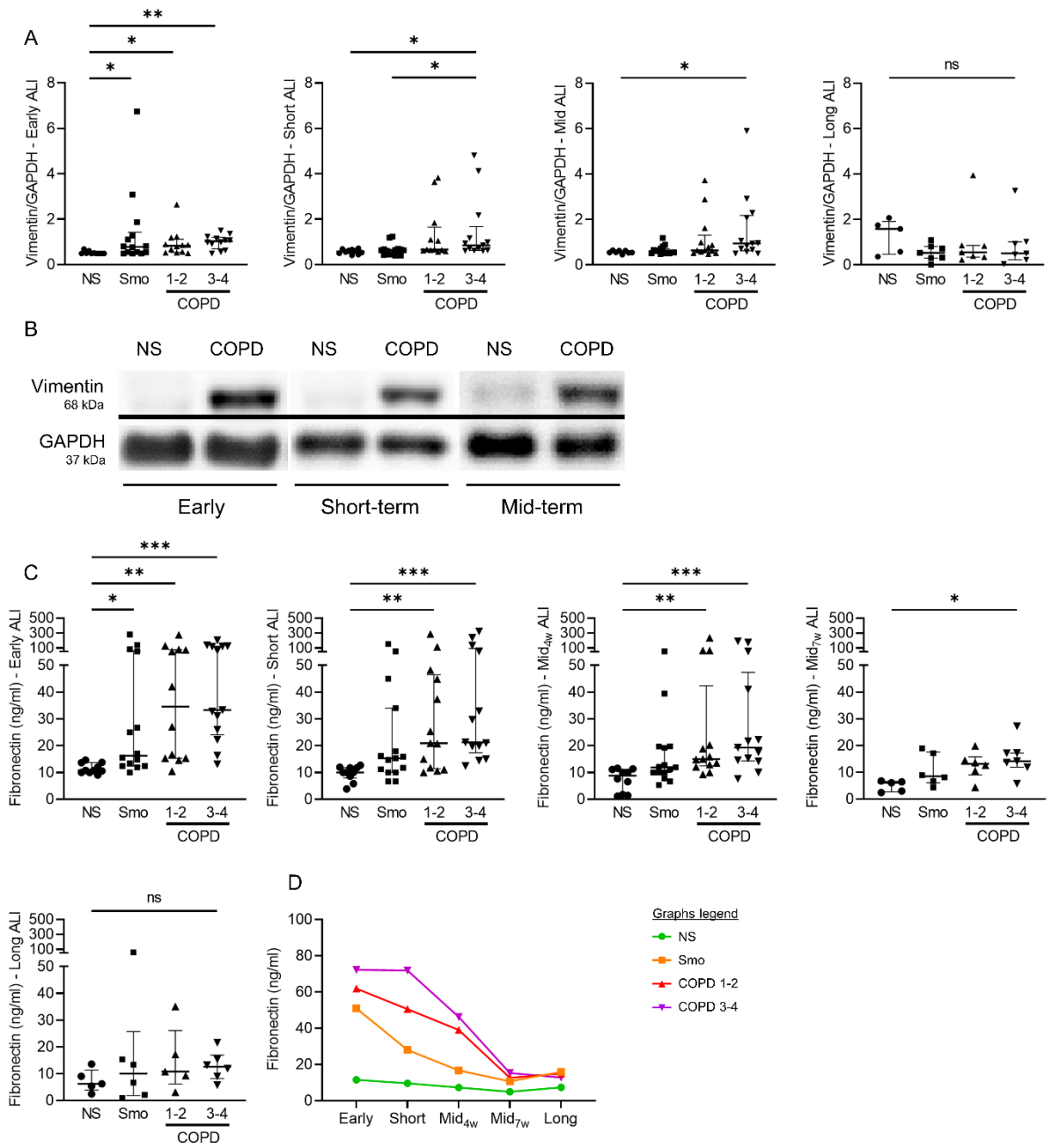

Figure 4 | COPD-related EMT features fade away in long-term ALI cultures.

A. Increased vimentin expression disappears early in smokers' ALI AE, but persists up to mid-term cultures in (very) severe COPD AE.
B. Illustrative gels from non-smokers and very severe COPD-derived AE in early, short-term and mid-term ALI cultures, illustrating the vimentin increased content in COPD.
C. Increased fibronectin release disappears in early ALI culture from smokers, in mid-term (4 weeks) cultures from mild-to-moderate COPD patients, while it persists up to later mid-term cultures (7 weeks) in (very) severe COPD AE.
D. Longitudinal analysis of the fibronectin release over time. °, # < 0.05; § < 0.01, mixed model analysis.
*, **, *** indicate p-values of less than 0.05, 0.01, and 0.001, respectively (analysed using the Kruskal-Wallis test followed by Dunn's post-hoc test, except for D, mixed model). Bars indicate median ± interquartile range, except for D, mean ± SEM. °: CT NS *versus* Smo; #: CT NS *versus* COPD 1-2, §: CT NS *versus* COPD 3-4.
AE, airway epithelium; ALI, air-liquid interface; COPD, chronic obstructive pulmonary disease; GAPDH, glyceraldehyde-3-phosphate dehydrogenase; NS, non-smokers; ns, not significant; SEM, standard error of the mean; Smo, smokers; w, weeks.

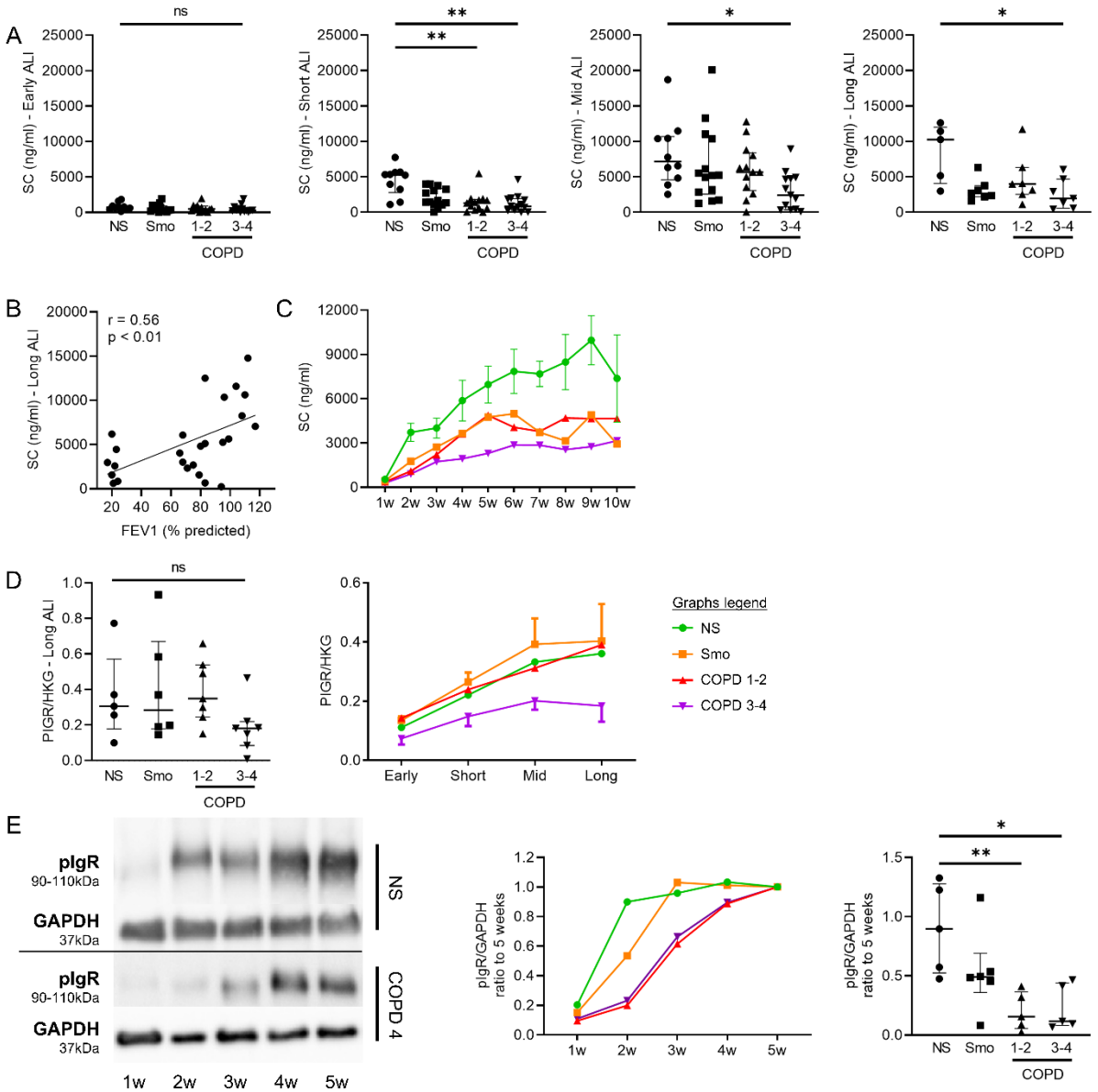

Figure 5 | Impaired polarity, witnessed by a disruption and a delayed acquisition of the PIGR/SC system, is imprinted in the COPD AE.

A. SC apical release in ALI-AE from smokers and COPD patients is decreased as compared with non-smokers, from short-term ALI-AE up to long-term ALI-AE.

B. SC decreased release in the COPD AE moderately correlates with the disease severity, witnessed by the FEV1.

C. Longitudinal analysis of SC apical release demonstrates a decreased release in smokers and mild-to-moderate COPD, as compared with non-smokers. This impaired SC production is enhanced in (very) severe COPD AE. °, #, § < 0.0001; £, ¶ < 0.001, mixed model analysis.

D. *PIGR* mRNA abundance is not significantly decreased in (very) severe COPD ALI-AE at separate time-points, as depicted here in long-term ALI cultures (see also Figure S4B), but longitudinal analysis shows a significant decrease in *PIGR* expression in (very) severe COPD AE as compared with non-smokers, smokers and mild-to-moderate COPD. £, ¶ < 0.001, § < 0.01, mixed model analysis.

E. pIgR acquisition is delayed during the differentiation of the AE in COPD as compared with non-smokers, as represented at 2 weeks ALI culture, and catches it up only after 4 weeks.

*, **, ***, **** indicate p-values of less than 0.05, 0.01, 0.001, and 0.0001, respectively (analyzed using the Kruskal-Wallis test followed by Dunn's post-hoc test, except for longitudinal analysis in B and C, mixed model). Bars indicate median ± interquartile range, except for longitudinal analysis in B and C, mean ± SEM.

°: CT NS *versus* Smo; #: CT NS *versus* COPD 1-2, §: CT NS *versus* COPD 3-4, £: CT S *versus* COPD 3-4, ¶: COPD 1-2 *versus* COPD 3-4.

AE, airway epithelium; ALI, air-liquid interface; COPD, chronic obstructive pulmonary disease; FEV1, forced expired volume in 1 second; GAPDH, glyceraldehyde-3-phosphate dehydrogenase; HKG, housekeeping genes;

NS, non-smokers; ns, not significant; pIgR, polymeric immunoglobulin receptor; PV, predicted values; SC, secretory component; SEM, standard error of the mean; Smo, smokers; w, weeks.

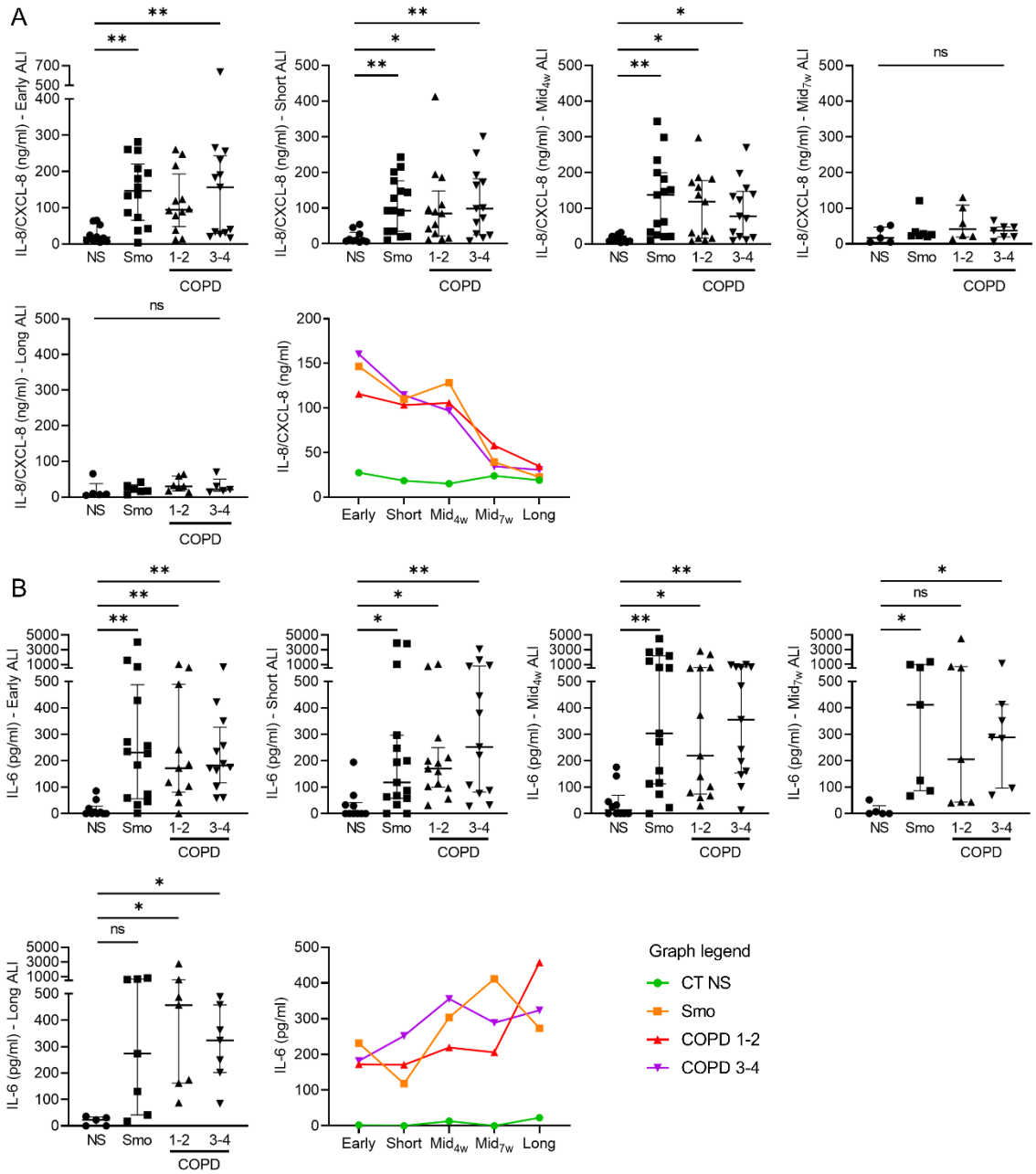

Figure 6 | Epithelial release of inflammatory cytokines partly persists in COPD AE.

A. IL-8/CXCL-8 production by the reconstituted ALI-AE is increased in early, short-term and mid-term ALI-AE from and COPD patients, but disappears afterwards, although a non-significant upward trend persists. °, #, § < 0.0001, mixed model analysis.

B. IL-6 production by the reconstituted ALI-AE is increased in smokers and COPD and persists in long-term cultures.

*, ** indicate p-values of less than 0.05 and 0.01, respectively (analysed using the Kruskal-Wallis test followed by Dunn's post-hoc test, except for longitudinal analysis, mixed model). Bars indicate median ± interquartile range, except for longitudinal analysis, mean. °, #, § < 0.0001, mixed model analysis.

°: CT NS *versus* Smo; #: CT NS *versus* COPD 1-2, §: CT NS *versus* COPD 3-4.

AE, airway epithelium; ALI, air-liquid interface; COPD, chronic obstructive pulmonary disease; IL, interleukin; NS, non-smokers; ns, not significant; SEM, standard error of the mean; Smo, smokers; w, weeks.

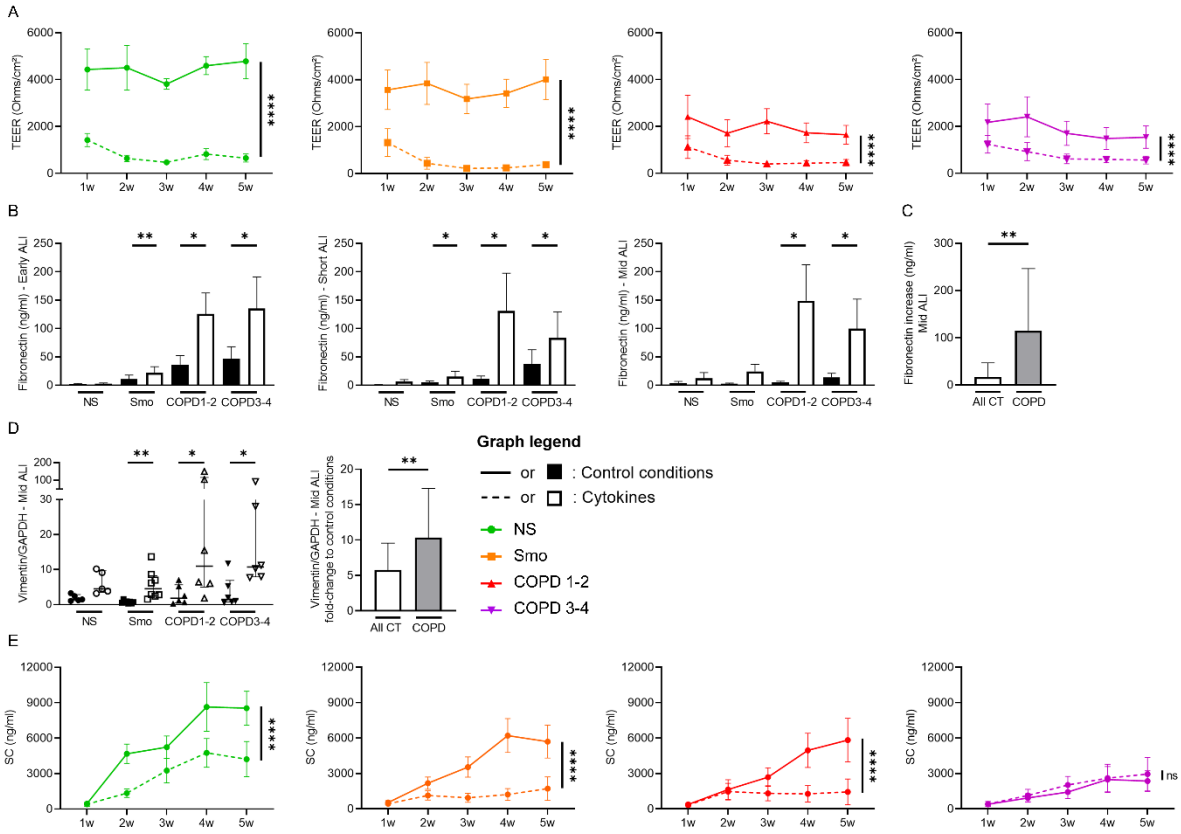

Figure 7 | Cytokine activation triggers COPD-like epithelial changes.
A. Epithelial inflammation, driven by exogenous TNF-α, IL-1β and IL-6, induces barrier dysfunction, witnessed by a dramatic decrease in TEER that is present in each group (NS, Smo, COPD 1-2, COPD 3-4).
B-D. Cytokine-induced epithelial inflammation induces EMT in smokers and COPD-derived ALI AE, witnessed by increased fibronectin release in early, short-term and mid-term cultures (B) and vimentin expression in mid-term cultures (D). The absolute increase in fibronectin and vimentin was significantly higher in mid-term COPD AE than in controls (pooled smokers and non-smokers) (C, D).
E. Cytokine-induced epithelial inflammation deteriorates the epithelial polarity, witnessed by the SC apical release. No difference was seen in (very) severe COPD, due to low baseline levels.
*, **, ***, **** indicate p-values of less than 0.05, 0.01, 0.001, and 0.0001, respectively (analyzed using the Mann-Whitney test for B, C and D, and a mixed model for A and E). Bars indicate median ± interquartile range for B, C and D, and mean ± SEM for A and E.
AE, airway epithelium; ALI, air-liquid interface; COPD, chronic obstructive pulmonary disease; CT, controls; EMT, epithelial-to-mesenchymal transition; GAPDH, glyceraldehyde-3-phosphate dehydrogenase; IL, interleukin; NS, non-smokers; ns, not significant; SC, secretory component; SEM, standard error of the mean; Smo, smokers; TEER, transepithelial electric resistance; TNF-α, tumor necrosis factor α; w, weeks.

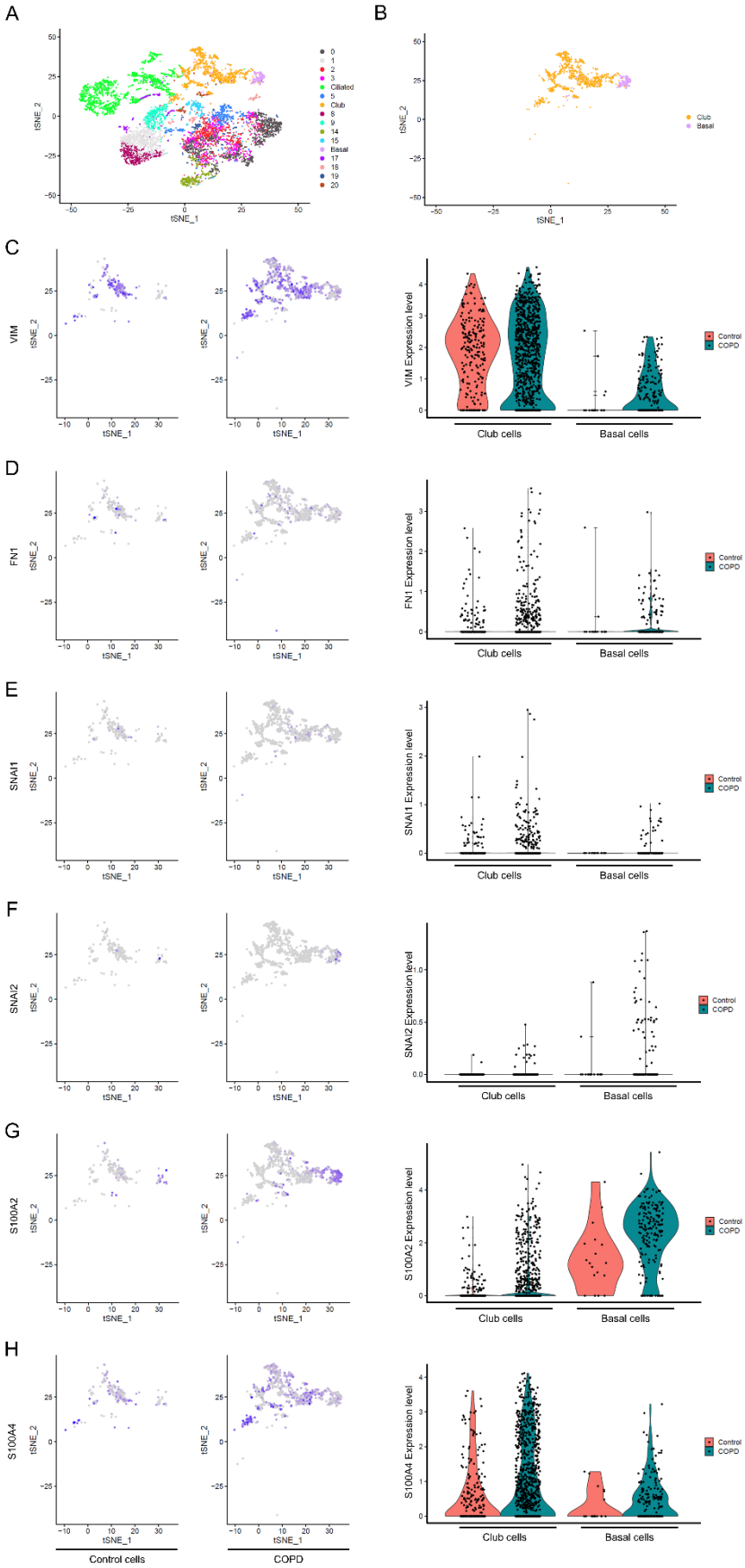

Figure 8 | EMT-related genes in airway progenitor cells.
A. t-SNE plot displaying the major clusters of human distal lung cells.
B. t-SNE plot isolating clusters of basal and club cells, that were further analysed.

C. Left graphs: t-SNE showing the expression of *VIM* in basal and club cells of controls and COPD patients. Right graphs: violin plots summarizing transcription levels of *VIM* in club and basal cells from controls (red violins) and COPD patients (blue violins).
D. Left graphs: t-SNE showing the expression of *FN1* in basal and club cells of controls and COPD patients. Right graphs: violin plots summarizing transcription levels of *FN1* in club and basal cells from controls (red violins) and COPD patients (blue violins).
E. Left graphs: t-SNE showing the expression of *SNAI1* in basal and club cells of controls and COPD patients. Right graphs: violin plots summarizing transcription levels of *SNAI1* in club and basal cells from controls (red violins) and COPD patients (blue violins).
F. Left graphs: t-SNE showing the expression of *SNAI2* in basal and club cells of controls and COPD patients. Right graphs: violin plots summarizing transcription levels of *SNAI2* in club and basal cells from controls (red violins) and COPD patients (blue violins).
G. Left graphs: t-SNE showing the expression of *S100A42* in basal and club cells of controls and COPD patients. Right graphs: violin plots summarizing transcription levels of *S100A2* in club and basal cells from controls (red violins) and COPD patients (blue violins).
H. Left graphs: t-SNE showing the expression of *S100A4* in basal and club cells of controls and COPD patients. Right graphs: violin plots summarizing transcription levels of *S100A4* in club and basal cells from controls (red violins) and COPD patients (blue violins).